Cerebral Cortex January 2016;26:180–191
doi:10.1093/cercor/bhu190
Advance Access publication August 21, 2014

Distinct Physiological Effects of Dopamine D4 Receptors on Prefrontal Cortical Pyramidal Neurons and Fast-Spiking Interneurons

Ping Zhong[1,2] and Zhen Yan[1,2]

[1]Department of Physiology and Biophysics, School of Medicine and Biomedical Sciences, State University of New York at Buffalo, Buffalo, NY 14214, USA and [2]VA Western New York Healthcare System, Buffalo, NY, USA

Address correspondence to Zhen Yan. Email: zhenyan@buffalo.edu

Dopamine D_4 receptor (D_4R), which is strongly linked to neuropsychiatric disorders, such as attention-deficit hyperactivity disorder and schizophrenia, is highly expressed in pyramidal neurons and GABAergic interneurons in prefrontal cortex (PFC). In this study, we examined the impact of D_4R on the excitability of these 2 neuronal populations. We found that D_4R activation decreased the frequency of spontaneous action potentials (sAPs) in PFC pyramidal neurons, whereas it induced a transient increase followed by a decrease of sAP frequency in PFC parvalbumin-positive (PV+) interneurons. D_4R activation also induced distinct effects in both types of PFC neurons on spontaneous excitatory and inhibitory postsynaptic currents, which drive the generation of sAP. Moreover, dopamine substantially decreased sAP frequency in PFC pyramidal neurons, but markedly increased sAP frequency in PV+ interneurons, and both effects were partially mediated by D_4R activation. In the phencyclidine model of schizophrenia, the decreasing effect of D_4R on sAP frequency in both types of PFC neurons was attenuated, whereas the increasing effect of D_4R on sAP in PV+ interneurons was intact. These results suggest that D_4R activation elicits distinct effects on synaptically driven excitability in PFC projection neurons versus fast-spiking interneurons, which are differentially altered in neuropsychiatric disorder-related conditions.

Keywords: D4 receptors, dopamine, interneurons, prefrontal cortex, synaptically driven excitability

Introduction

The neocortex is composed of 2 major neuronal populations: glutamatergic pyramidal neurons and γ-aminobutyric acid (GABA)ergic interneurons. Although GABAergic interneurons only account for approximately 20% of the cortical neuronal population (Hendry et al. 1987), they are critical elements of cortical circuits by providing feedforward and feedback inhibition and generating synchronous and rhythmic network activity (McBain and Fisahn 2001). Selective alterations in GABAergic local-circuit neurons, GABA synthesis enzyme GAD67, GABA content, and $GABA_A$ receptors have been discovered in prefrontal cortex (PFC) of schizophrenic patients (Akbarian et al. 1995; Woo et al. 1998; Volk et al. 2000, 2002; Hashimoto et al. 2003; Lewis et al. 2005), suggesting that impairments in GABAergic inhibition in the PFC network might contribute to the aberrant neuronal synchrony and disrupted working memory in schizophrenia (Spencer et al. 2003; Lewis et al. 2012).

Cortical GABAergic interneurons are heterogeneous in terms of morphological features, circuit connections, electrophysiological characteristics, and protein expression patterns (Hestrin 1993; Geiger et al. 1995; Markram et al. 2004; Cruikshank et al. 2007). Several calcium-binding proteins, such as parvalbumin, calbindin, and calrectinin, which are highly expressed in cortical GABAergic interneurons, are often used as markers to distinguish cortical interneurons (Kawaguchi and Kubota 1993, 1998; Cauli et al. 1997). Parvalbumin-positive (PV+) interneurons have received special attentions because they possess powerful output synapses localized to the perisomatic region of target cells (Kawaguchi and Kubota 1993, 1998) and form dense gap-junctional connectivity with one another (Kawaguchi and Kubota 1997; Galarreta and Hestrin 1999). PV+ interneuron dysfunction has been hypothesized to play a role in the pathogenesis of various neurological and psychiatric disorders, including schizophrenia, autism, and epilepsy (Beasley et al. 2002; Levitt et al. 2004; Lewis et al. 2005, 2012; Torrey et al. 2005; Walsh et al. 2008).

Functions of PFC are strongly influenced by dopamine signaling (Sawaguchi and Goldman-Rakic 1991; Williams and Goldman-Rakic 1995; Wang et al. 2004; Vijayraghavan et al. 2007). One of the dopamine receptor subtypes, the D_4 receptor (D_4R), has been found to be enriched in PFC GABAergic interneurons and pyramidal neurons (Mrzljak et al. 1996; Wedzony et al. 2000). The D_4 receptor is implicated in schizophrenia because of its high affinity to the uniquely effective antipsychotic drug clozapine (Van Tol et al. 1991; Kapur and Remington 2001). Moreover, D_4 gene polymorphisms are strongly linked to attention deficit-hyperactivity disorder (LaHoste et al. 1996; Rowe et al. 1998; El-Faddagh et al. 2004; Li et al. 2006). In this study, we examined the impact of D_4 receptors on cellular excitability, which is driven by the integration of excitatory and inhibitory synaptic inputs, in PFC pyramidal neurons and PV+ interneurons from normal animals and a model of schizophrenia.

Methods

Animals and Cell Identification

Transgenic mice expressing the enhanced green fluorescent protein (EGFP) in interneurons containing parvalbumin (G42, Jackson Lab.) were used in this study. G42 mice were engineered by the genomic incorporation of a 200-kb GAD1 bacterial artificial chromosome fused to the EGFP coding sequence (Chattopadhyaya et al. 2004; Gibson et al. 2009). Cortical expression of GFP-positive neurons was restricted to Layers 2/3, 5, and 6, with occasional expression in Layer 4 (Okaty et al. 2009). D_4R knockout (KO) mice (Rubinstein et al. 1997, 2001) were kindly provided by Dr Grandy (Oregon Health Sciences University, Portland, OR). PV mice (G42) were cross-bred with homozygous D_4R KO mice to get D_4R-deficient, PV+ neurons (GFP+) for recordings in some experiments.

Subchronic (5-day) phencyclidine (PCP) treatment was used to generate the mouse model of schizophrenia, as previously described (Javitt and Zukin 1991; Arvanov and Wang 1999; Wang et al. 2006). Mice were i.p. injected (once daily) with PCP (Sigma) at a dose of 5 mg/kg for 5 days and sacrificed 24 h after the last injection.

Electrophysiological Recordings in Slices

Brain slices from 1- to 2-month-old mice were prepared as described previously (Zhong et al. 2003; Yuen et al. 2010). All experiments were carried out with the approval of State University of New York at Buffalo Animal Care Committee. In brief, mice were first anesthetized by inhaling Halothane (Sigma) for approximately 30 s and decapitated quickly. Brains were quickly removed and cut into coronal slices (300 μm) using Vibratome (Leica VP1000S) in the ice-cold sucrose solution (in mM: 234 sucrose, 4 $MgSO_4$, 2.5 KCl, 1 NaH_2PO_4, 0.1 $CaCl_2$, 15 HEPES, 11 glucose, pH 7.4). Slices were then incubated for 1–3 h at room temperature (22–24 °C) in artificial cerebrospinal fluid (ACSF) (in mM: 130 NaCl, 26 $NaHCO_3$, 1 $CaCl_2$, 2 $MgCl_2$, 3 KCl, 10 glucose, 1.25 NaH_2PO_4) bubbled with 95% O_2, 5% CO_2.

Whole-cell patch-clamp experiments were performed with a Multiclamp 700A amplifier and Digidata1322A data acquisition system (Molecular Devices). Neurons were visualized with the infrared differential interference contrast video microscopy. Large neurons with the triangle-shaped soma in the deep layer (Layer 5) of PFC were selected as pyramidal neurons. GFP-positive interneurons from PV mice (G42) were visualized with an upright microscope illuminated with a xenon lamp and equipped with a ×40 water-immersion lens and EGFP filters. Recording electrodes were pulled from borosilicate glass capillaries (1.5/0.86 mm OD/ID) with a micropipette puller (Sutter Instrument Co., Model P-97) and had a resistance of 3–4 MΩ.

To record the spontaneous action potential (sAP), we used a modified ACSF that slightly elevated basal neuronal activity (in mM: 130 NaCl, 26 $NaHCO_3$, 2 $CaCl_2$, 0.5 $MgCl_2$, 3.5 KCl, 10 glucose, 1.25 NaH_2PO_4), which more closely mimics the ionic composition of brain interstitial fluid in situ (1.0–1.2 mM Ca^{2+}, 1 mM Mg^{2+}, and 3.5 mM K^+) (Sanchez-Vives and McCormick 2000; Maffei et al. 2004). Spontaneous action potential was induced and recorded in the whole-cell current clamp mode with the internal solution containing (in mM): 20 KCl, 100 K-gluconate, 10 HEPES, 4 Mg-ATP, 0.5 Na_2GTP, and 10 Na-phosphocreatine (Maffei and Turigiano 2008). This same internal solution was used for examining the passive membrane properties (see Table 1). Action potentials evoked by current injections were recorded in the whole-cell current clamp mode in regular ACSF (in mM: 130 NaCl, 26 $NaHCO_3$, 1 $CaCl_2$, 5 $MgCl_2$, 3 KCl, 10 glucose, 1.25 NaH_2PO_4). $GABA_AR$ antagonist Bicuculline (10 μM), AMPAR antagonist DNQX

Table 1
Membrane properties and spontaneous AP properties in PFC pyramidal neurons and PV+ interneurons

	PFC pyramidal neuron	PFC PV+ interneuron
Resting potential (mV)	−63.8 ± 0.8	−69.5 ± 1.9
Spike threshold (mV)	−45.9 ± 0.9	−46.1 ± 1.0
Input resistance (MΩ)	238.2 ± 10.3	147.7 ± 8.8*
Spike amplitude (mV)	84.3 ± 1.8	65.3 ± 2.1*
Spike halfwidth (ms)	1.8 ± 0.1	0.8 ± 0.1*
Membrane capacitance (pF)	63.2 ± 2.1	36.2 ± 1.7*
Cell number	11	12

*$P < 0.05$, K–W test.

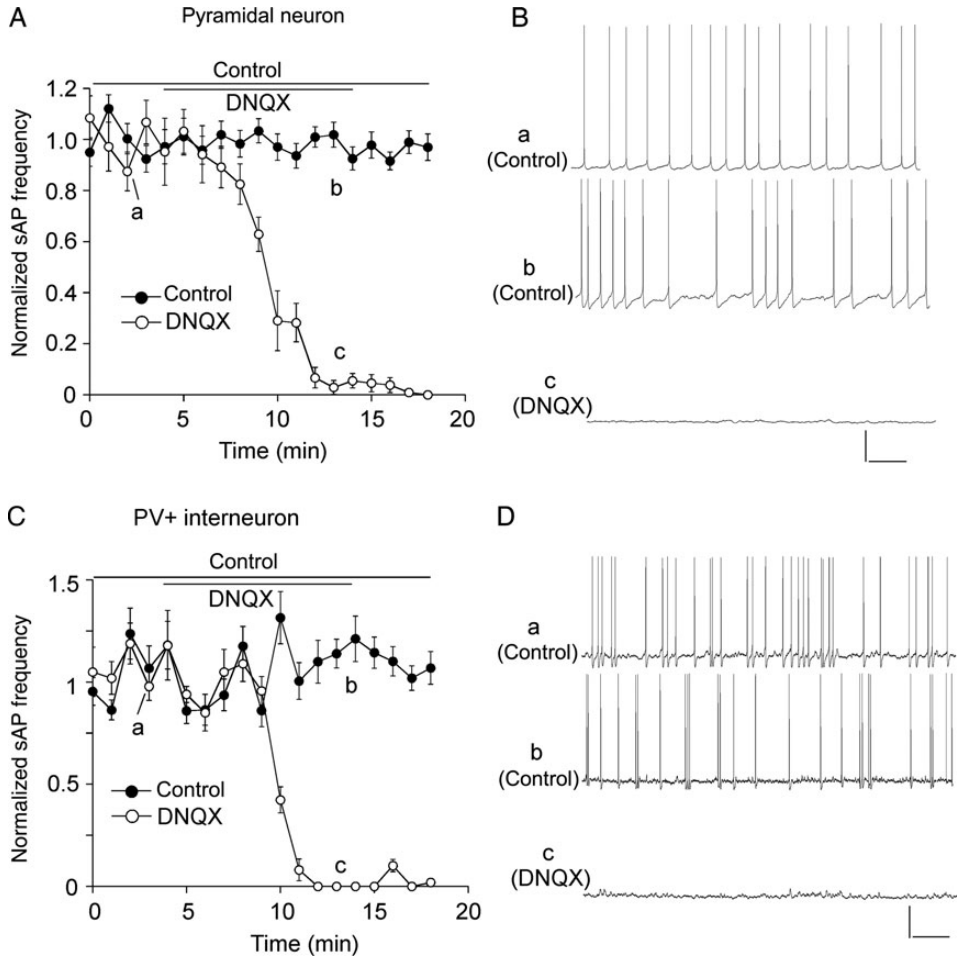

Figure 1. Spontaneous action potentials were dependent on AMPAR-mediated synaptic transmission. (*A*,*C*) The plot of normalized frequency of sAPs before and after the application of AMPAR antagonist DNQX (50 μM) in PFC pyramidal neurons (*A*) and PV+ interneurons (*C*). (*B*,*D*) Representative traces of sAPs at time points (denoted by *a*–*c*) in plots A and C. Scale bars: 20 mV, 1 s.

(50 μM), and NMDAR antagonist APV (50 μM) were added to the external solution. Synaptic currents (sEPSC, mEPSC, sIPSC, and mIPSC) were recorded in the whole-cell voltage-clamp mode (clamped at −70 mV) in regular ACSF. Tetrodotoxin (1 μM) was added to ACSF during miniature synaptic current recordings. The internal solution for EPSC contained (in mM): 130 Cs-methanesulphonate, 10 CsCl, 4 NaCl, 10 HEPES, 1 $MgCl_2$, 5 EGTA, 2 QX-314, 12 phosphocreatine, 5 MgATP, 0.5 Na_2GTP, pH 7.2–7.3, 265–270 mosM. The internal solution for IPSC contained (in mM): 100 CsCl, 30 N-methyl-D-glucamine, 10 HEPES, 4 NaCl, 1 $MgCl_2$, 5 EGTA, 2 QX-314, 12 phosphocreatine, 5 MgATP, 0.5 Na_2GTP, pH 7.2–7.3, 265–270 mOsM. Tight seals (2–10 GΩ) were obtained by applying negative pressure. The membrane was disrupted with additional suction, and the whole-cell configuration was obtained. The access resistances ranged from 10 to 15 MΩ and did not change >10% during the recording.

Data Analysis

Data were acquired using the software pClampex 9.2 (Molecular Device). Data-sampling frequency was 10 kHz, and filtering frequency was 1 kHz. Data analyses were performed with the Clampfit software (Molecular Devices), Mini Analysis Program (Synaptosoft), and KaleidaGraph software. Neuronal input resistance was determined by dividing the difference in membrane voltage in response to a hyperpolarizing current pulse that caused a voltage deflection (Yang et al. 1996). Resting potentials were measured just after the patched membrane was ruptured by suction (Kawaguchi 1995). Resting membrane potential, input resistance, and membrane capacitance were measured in regular ACSF. The sAP parameters were obtained by measuring and averaging 5 continuous action potentials at the stable state, as previously described (Cauli et al. 1997).

The baseline frequency of sAP was approximately1–2 Hz for pyramidal neurons and 2–5 Hz for PV+ interneurons. The inter-spike membrane potential was approximately −58 mV (pyramidal) or approximately −56 mV (PV+) either without a holding current or with a small (<50 pA) adjusting current (positive DC). The data were normalized to the average of baseline in control conditions before the drug applications.

In the analysis of spontaneous postsynaptic currents, we set up a threshold of amplitude for detecting the synaptic events. The threshold should be approximately 2 root mean squares of control baseline noise (Beierlein et al. 2003). Accordingly, we set the threshold of sEPSC at 6 pA and the threshold of sIPSC at 8 pA. "Big" events were defined as those with amplitudes larger than the average baseline values of all events. "Big" events generally account for 30–40% of total events.

Agents such as PD168077, GBR-12909, sulpiride, SCH23390, L-745870, and dopamine were purchased from Tocris or Sigma. Stocks were made up as concentrated stocks in water or DMSO and stored at −20°C. Stocks were thawed and diluted immediately before use.

All data are expressed as the mean ± SEM. Mann–Whitney *U* tests (two-tailed, unpaired) were used to determine the significance of effects on action potentials. Kolmogorov–Smirnov (K–S) tests (two-tailed, unpaired) were used to determine the significance of effects on sEPSC, mEPSC, sIPSC, or mIPSC. Since the data distribution in different animals was often found to be non-normal, non-parametric statistical analysis was performed with Kruskal–Wallis (K–W) tests to compare the effects between different groups.

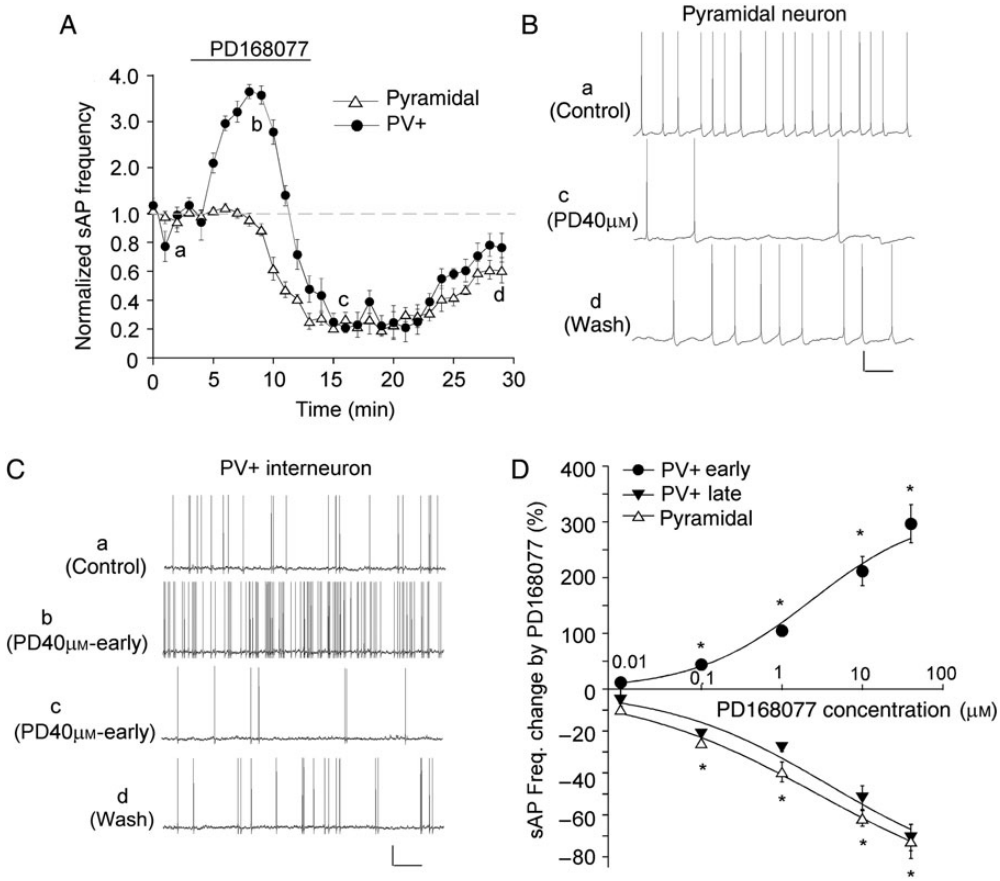

Figure 2. D_4R agonist PD168077 induced different effects on sAP frequency in PFC pyramidal neurons and PV+ interneurons. (*A*) The time course of normalized sAP frequency showing the effect of PD168077 (40 μM) in PFC pyramidal neurons (triangle unfilled) and PV+ interneurons (round filled). (*B*,*C*) Representative traces of sAP at different time points (denoted by *a*–*d*) in plot A. Scale bars: 20 mV, 1 s. (*D*) Dose–response data and fitted curves showing the percentage changes in sAP frequency by different concentrations of PD168077 in PFC pyramidal neurons and PV+ interneurons. *$P < 0.01$.

Results

D4R Activation Induced Distinct Effects on Spontaneous Action Potentials in PFC Pyramidal Neurons and Parvalbumin-Positive Interneurons

Compared with PFC pyramidal neurons, PV+ interneurons exhibited a lower input resistance and a smaller membrane capacitance (Table 1). The sAP in both neuronal types also exhibited different characteristics, with shorter spike half-time and smaller spike amplitude in PV+ interneurons than in pyramidal neurons (pyramidal: 1.8 ± 0.1 ms, 84.3 ± 1.8 mV, $n = 11$; PV+: 0.8 ± 0.05 ms, 69.7 ± 1.4 mV, $n = 12$, $P < 0.05$, K–W test). Application of AMPAR antagonist DNQX (50 μM, 10 min) totally abolished sAP in both types of PFC neurons (Fig. 1*A–D*), indicating that the sAPs are determined by synaptic transmission.

Next, we examined the effect of D_4R activation on sAPs in PFC pyramidal neurons and PV+ interneurons. As shown in Figure 2*A–C*, application of the specific D_4R agonist PD168077 (40 μM, 10 min) significantly decreased sAP frequency in pyramidal neurons. It took approximately 5 min to induce an apparent effect, and the reduction reached the maximal level at approximately 8th min. In PV+ interneurons, PD168077 (40 μM, 10 min) induced a large increase, followed by a delayed decrease, of sAP frequency. The early increasing effect started to occur at approximately 1.5th min during agonist application, reached the maximal level at approximately 4.5th min, and disappeared at approximately 7th min. The late decreasing effect started to occur at approximately 8th min, reached the maximal level at approximately 9th–10th min, sustained for 5–8 min after PD168077 termination, and disappeared after 15–20 min of washing.

We further examined the dose dependence of PD168077 effects on sAP in both types of PFC neurons. As shown in Figure 2*D*, in pyramidal neurons, PD168077 induced a dose-dependent reduction of sAP frequency (0.1 μM: 25.6 ± 1.9%, $n = 6$; 1 μM: 39.5 ± 4.8%, $n = 9$; 10 μM: 61.6 ± 3.8%, $n = 8$; 40 μM: 72.6 ± 8.2%, $n = 16$, $P < 0.01$, Mann–Whitney U test) with an EC_{50} of 2.9 μM. In PV+ interneurons, PD168077 induced a dose-dependent (EC_{50}: 2.3 μM) increase of sAP frequency in the early phase (0.1 μM: 44.3 ± 3.5%, $n = 6$; 1 μM: 104.4 ± 10.3%, $n = 9$; 10 μM: 211.7 ± 26.1%, $n = 10$; 40 μM: 296.8 ± 34.2%, $n = 15$, $P < 0.01$, Mann–Whitney U test), followed by a dose-dependent (EC_{50}: 3.7 μM) decrease of sAP frequency in the late phase (0.1 μM: 21.4 ± 1.3%, $n = 5$; 1 μM: 27.7 ± 2.1%, $n = 9$; 10 μM: 51.8 ± 5.6%, $n = 10$; 40 μM: 70.8 ± 8.2%, $n = 15$, $P < 0.01$, Mann–Whitney U test). The low dose of PD168077 (0.01 μM) had little effects in either of the neuronal types.

To determine whether activation of endogenous D_4 receptors also affects sAP, we applied the specific dopamine transporter inhibitor GBR-12909 (10 μM) to block the reuptake of dopamine. The $D_{2/3}$ antagonist sulpiride (5 μM) and $D_{1/5}$

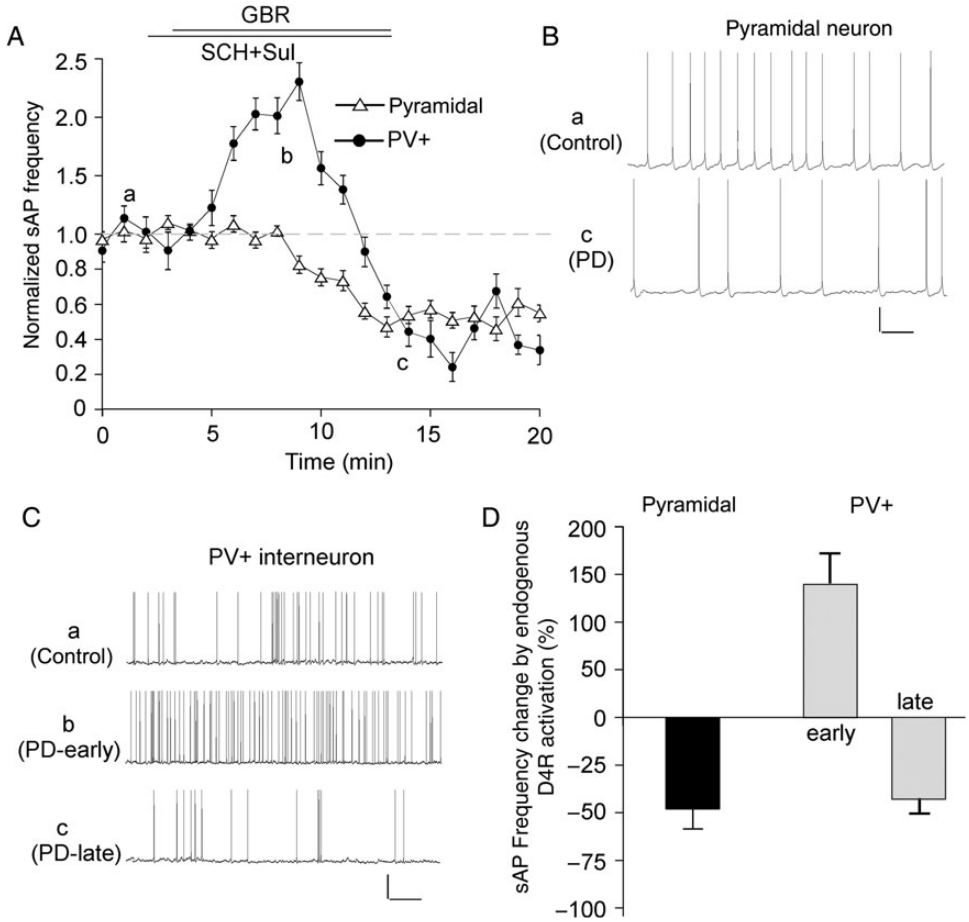

Figure 3. Endogenous D_4R activation induced different effects on sAP frequency in PFC pyramidal neurons and PV+ interneurons. (*A*) The time course of normalized sAP frequency showing the effect of dopamine transporter inhibitor GBR-12909 (10 μM), in the presence of $D_{1/5}$ antagonist SCH23390 (10 μM) and $D_{2/3}$ antagonist sulpiride (5 μM), in PFC pyramidal neurons (triangle unfilled) and PV+ interneurons (round filled). (*B,C*) Representative traces of sAP at different time points (denoted by *a–c*) in plot A. Scale bars: 20 mV, 1 s. (*D*) Bar graph summary of percentage change of sAP frequency by GBR-12909 (in the presence of SCH23390 and sulpiride) in PFC pyramidal neurons and PV+ interneurons.

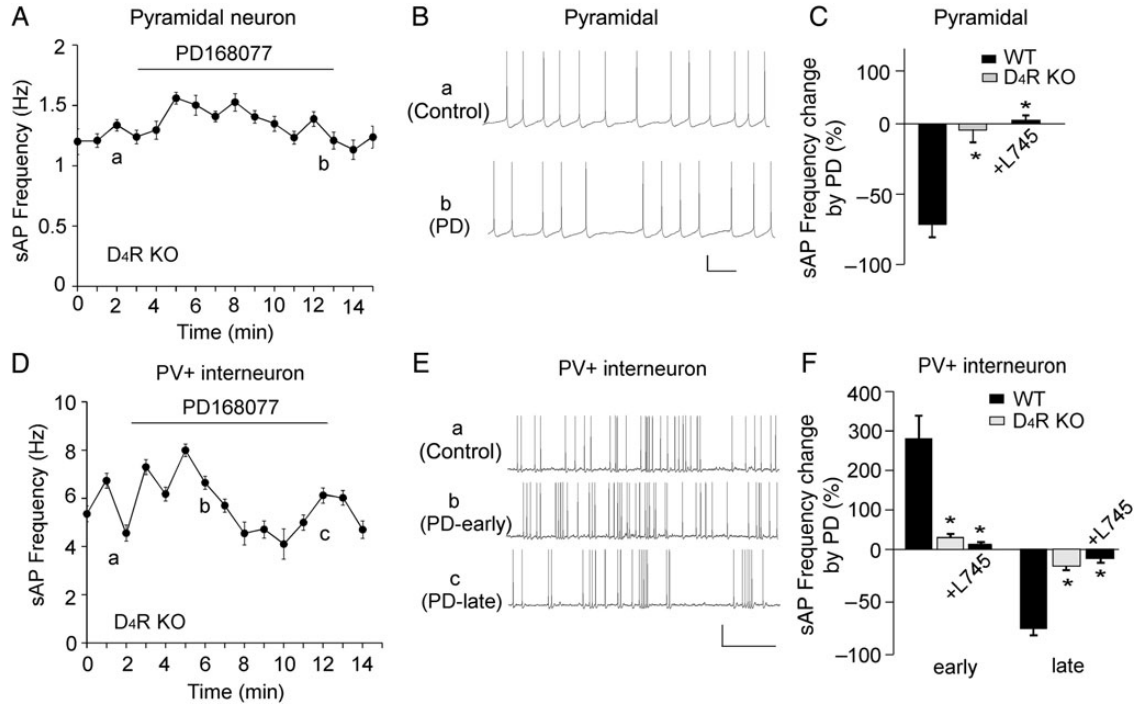

Figure 4. The effect of PD168077 on sAP frequency was mediated by D_4R activation. (*A*,*D*) The time course of sAP frequency showing the lack of effect of PD168077 (40 μM) in PFC pyramidal neurons (*A*) and PV+ interneurons (*D*) from D4R KO mice. (*B*,*E*) Representative traces of sAP at different time points (denoted by *a*–*c*) in plots A and D. Scale bars: 20 mV, 1 s. (*C*,*F*) Bar graph summary of percentage change of sAP frequency by PD168077 in PFC pyramidal neurons (*C*) and PV+ interneurons (*F*) from WT vs., D_4R KO mice, as well as the effect of PD168077 in the presence of D4 antagonist L745870 (20 μM) in WT mice. $^*P < 0.01$.

antagonist SCH23390 (10 μM) were co-applied to block the activation of non-D_4 dopamine receptors. As shown in Figure 3, GBR-12909 significantly decreased sAP frequency (48.2 ± 10.5%, $n = 6$, $P < 0.01$, Mann–Whitney U test) in pyramidal neurons, whereas it induced an initial increase (141.4 ± 30.1%, $n = 7$, $P < 0.01$, Mann–Whitney U test) and a delayed decrease (42.7 ± 7.6%, $n = 7$, $P < 0.01$, Mann–Whitney U test) of sAP frequency in PV+ interneurons, similar to what was seen with PD168077.

To further determine the involvement of D_4Rs, we recorded D_4R KO mice. As shown in Figure 4*A–C*, PD168077 failed to induce a significant effect on sAP frequency in pyramidal neurons from D_4R KO mouse [wild-type (WT): 71.5 ± 8.2% decrease, $n = 5$; KO: 4.5 ± 8.5% decrease, $n = 5$, $P < 0.01$, K–W test]. Moreover, the effect of PD168077 in WT mice was blocked by the D_4R antagonist L-745870 (20 μM, 6.4 ± 10.2% increase, $n = 7$, $P < 0.01$, K–W test, Fig. 4*C*). In PV+ interneurons from D_4R KO mice (Fig. 4*D–F*), the effects of PD168077 on sAP frequency were also significantly smaller than those in WT mice (WT: 278.6 ± 51.7% early increase, 74.1 ± 7.3% late decrease, $n = 5$; KO: 28.6 ± 4.5% early increase, 17.3 ± 2.7% late decrease, $n = 5$, $P < 0.01$, K–W test). In addition, L-745870 largely blocked the effects of PD168077 in PV+ interneurons (12.7 ± 3.1% early increase, 9.2 ± 2.4% late decrease, $n = 8$, $P < 0.01$, K–W test, Fig. 4*F*).

D4R Activation Induced Distinct Effects on Synaptic Currents in PFC Pyramidal Neurons and Parvalbumin-Positive Interneurons

Since sAP firing reflects circuit excitability induced by synaptic drives (Maffei et al. 2004), we examined the effect of PD168077 on spontaneous excitatory and inhibitory postsynaptic currents (sEPSC and sIPSC) in both types of PFC neurons. In PFC pyramidal neurons, when data from all events were analyzed, PD168077 (40 μM, 10 min) reduced the amplitude and frequency of sEPSC and sIPSC slightly, but not significantly (Table 2). However, from the traces and cumulative distributions of synaptic currents, we found PD168077-induced prominent changes in those "big" synaptic events (with amplitudes larger than the mean values) that are supposed to play a major role in driving sAP firing. In pyramidal neurons, PD168077 significantly reduced the amplitude and frequency of "big" sEPSC (amplitude: 23.4 ± 2.2%, frequency: 35.4 ± 3.8%, $n = 7$, $P < 0.05$, K–S test, Fig. 5*A*,*C*, Table 2) and "big" sIPSC (amplitude: 22.9 ± 1.8%, frequency: 30.6 ± 2.1%, $n = 7$, $P < 0.05$, K–S test, Fig. 5*B*,*C*, Table 2). We also examined the effect of PD168077 on miniature synaptic currents, a synaptic response resulting from quantal release of single glutamate vesicles. In PFC pyramidal neurons, PD168077 (40 μM, 10 min) significantly reduced the amplitude and frequency of mEPSC (Fig. 5*D*,*F*, amplitude: 19.8 ± 0.9%, frequency: 25.3 ± 1.8%, $n = 9$, $P < 0.05$, K–S test) and significantly decreased the amplitude, but not frequency, of mIPSC (Fig. 5*E*, *F*, amplitude: 21.3 ± 0.7%, $n = 8$, $P < 0.05$, K–S test). It suggests that D_4R activation may affect excitatory transmission via both pre- and post-synaptic mechanisms, whereas it influences inhibitory transmission mainly postsynaptically in pyramidal neurons. Thus, D4R activation decreases both excitatory and inhibitory synaptic transmission in pyramidal neurons, and the integrated results may cause the decrease of sAP frequency.

In PV+ interneurons, the effects of PD168077 (40 μM, 10 min) on sEPSC and sIPSC were not statistically significant when data from all events were analyzed (Table 2). However, PD168077 induced a significant time-dependent biphasic effects on "big" sEPSC (Fig. 5*G*,*I*, early increase: 22.1 ± 1.4%

Table 2

Spontaneous EPSC and IPSC amplitudes and event numbers before (control) and after PD168077 application in PFC pyramidal neurons and PV+ interneurons

Pyramidal	Total		Big		Total		Big	
	Amplitude (pA)		Amplitude (pA)		Events (1 min)		Events (1 min)	
	Control	PD	Control	PD	Control	PD	Control	PD
sEPSC								
Cell 1	10.5	9.3	13.9	11.1	231	205	72	40
Cell 2	10.8	9.9	14.8	11.9	126	110	49	35
Cell 3	11.1	10.6	16.3	13.1	305	279	95	69
Cell 4	13.4	11.2	18.5	12.5	189	161	68	32
Cell 5	12.1	10.2	19.4	15.4	210	182	69	47
Cell 6	9.8	8.3	13.5	10.8	119	102	43	32
Cell 7	13.6	12.1	17.7	12.1	172	165	65	41
sIPSC								
Cell 1	15.6	13.5	23.7	19.1	358	317	129	95
Cell 2	21.6	18.4	32.5	25.3	452	392	178	119
Cell 3	19.4	17.4	29.8	24.1	268	236	86	60
Cell 4	18.7	17.2	31.7	26.6	327	295	117	90
Cell 5	16.3	14.5	27.2	19.2	294	253	105	68
Cell 6	20.1	18.2	30.4	22.1	392	346	141	103
Cell 7	19.7	16.8	28.1	20.6	303	310	119	72

PV+	Total			Big			Total			Big		
	Amplitude(pA)			Amplitude(pA)			Events (1 min)			Events (1 min)		
	Control	early	late	Control	early	late	Control	early	late	Control	early	late
sEPSC												
Cell 1	16.5	18.1	14.2	26.5	31.6	20.1	402	443	351	129	171	100
Cell 2	14.3	15.1	12.6	23.7	28.0	19.4	347	377	307	111	147	78
Cell 3	17.8	20.6	16.9	26.3	33.6	21.5	289	328	266	97	144	78
Cell 4	15.6	16.6	13.5	23.4	27.7	19.1	341	365	294	123	155	88
Cell 5	15.7	17.8	15.0	23.9	29.7	19.6	325	364	299	106	154	84
Cell 6	17.2	18.9	15.3	26.4	32.1	21.5	344	389	332	113	139	81
Cell 7	18.3	19.8	16.6	28.3	35.5	22.2	433	488	411	138	194	103
sIPSC												
Cell 1	14.2	12.5	15.2	25.1	18.0	30.2	364	319	416	117	88	174
Cell 2	15.1	14.1	17.2	24.1	19.3	32.4	369	339	409	123	76	173
Cell 3	14.3	13.2	16.1	24.6	19.4	30.4	236	214	259	84	48	108
Cell 4	17.6	15.2	19.0	27.7	19.1	33.1	128	111	145	43	29	66
Cell 5	14.8	13.2	16.2	26.5	20.6	32.1	168	158	180	57	44	84
Cell 6	16.9	15.6	18.1	27.7	21.9	32.6	328	298	401	98	64	138
Cell 7	18.2	17.2	20.8	31.2	24.8	35.7	378	334	434	121	83	159

Averaged values of the total synaptic events and the subpopulation of "big" synaptic events (with amplitudes bigger than the mean) in each cell are included.

[amplitude], 35.5 ± 3.6% [frequency]; late decrease: 19.6 ± 0.9% [amplitude], 24.9 ± 1.5% [frequency], $n = 7$, $P < 0.05$, K–S test, Table 2) and "big" sIPSC (Fig. 5*H*,*I*, early decrease: 23.4 ± 1.7% [amplitude], 32.5 ± 2.7% [frequency]; late increase: 21.6 ± 2.4% [amplitude], 41.6 ± 3.5% [frequency], $n = 7$, $P < 0.05$, K–S test, Table 2). Moreover, PD168077 significantly increased the frequency, but not amplitude, of mEPSC in the early phase and significantly decreased the amplitude, but not frequency, of mEPSC in the late phase (Fig. 5*J*,*L*, early increase: 46.3 ± 4.7% [frequency], late decrease: 24.2 ± 1.9% [amplitude], $n = 9$, $P < 0.05$, K–S test), suggesting that the effect of D_4R on excitatory transmission may be presynaptic in the early phase and postsynaptic in the late phase. For mIPSC in PV+ interneurons, PD168077 did not significantly change the amplitude or frequency of mIPSC in the early phase but significantly increased the amplitude and frequency in the late phase (Fig. 5*K*,*L*, 25.1 ± 2.1% [amplitude], 67.2 ± 10.8% [frequency], $n = 10$, $P < 0.05$, K–S test), suggesting that D_4R induces a delayed potentiation of inhibitory transmission via both pre- and post-synaptic mechanisms. Thus, in PV+ interneurons, the initial increase of excitatory drive and decrease of inhibitory drive may be responsible for the early increase of sAP frequency, whereas the delayed decrease of excitatory drive and increase of inhibitory drive may lead to the lower sAP frequency in the later phase of D_4R activation.

D4R Activation did not Affect Intrinsic Excitability in PFC Pyramidal Neurons and Parvalbumin-Positive Interneurons

The effect of D_4R activation on sAPs could be due to the D_4R-induced changes in synaptic transmission or intrinsic membrane properties. To test this, we examined the action potential induced by injected depolarizing current steps in the presence of excitatory and inhibitory synaptic blockers. As shown in Figure 6, PD168077 (40 μM, 10 min) did not induce any significant changes in the frequency of evoked action potential in both types of PFC neurons (pyramidal: 3.7 ± 1.3% decrease, $n = 9$; PV+: 4.1 ± 1.8% increase, $n = 8$, $P > 0.05$, Mann–Whitney U test). It suggests that the D_4R regulation of sAP relies on the changes in PFC synaptic transmission.

Dopamine Induced Distinct Effects on Spontaneous Action Potentials in PFC Pyramidal Neurons and Parvalbumin-Positive Interneurons, which was Partially Regulated by D_4Rs

Next, we examined the impact of dopamine on sAP in PFC neurons and the involvement of D_4R. As shown in Figure 7*A*,*B*, application of dopamine (1 μM, 10 min) significantly decreased sAP frequency in pyramidal neurons (68.7 ± 5.8%, $n = 10$, $P < 0.01$, Mann–Whitney U test, Fig. 7*E*),

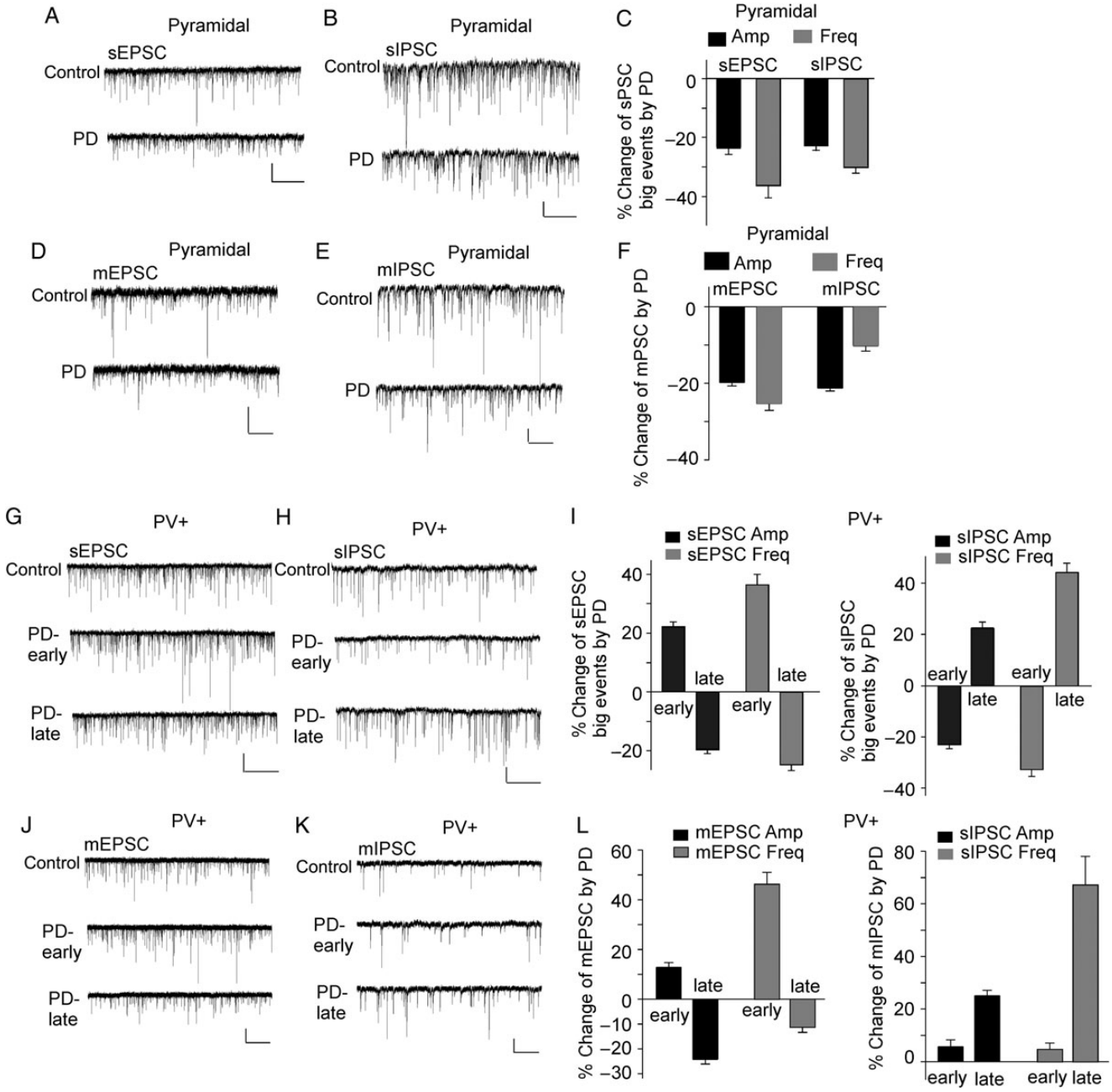

Figure 5. D_4R agonist PD168077 induced different effects on excitatory and inhibitory synaptic transmission in PFC pyramidal neurons and PV+ interneurons. (*A–E*) Representative traces of sEPSC (*A*), sIPSC (*B*), mEPSC (*D*), and mIPSC (*E*) before and after PD168077 (40 μM, 10 min) treatment in PFC pyramidal neurons. Scale bars: 20 pA, 5 s (*A*,*B*), 2 s (*D*,*E*). (*C*,*F*) Bar graph summary of the percentage change in the spontaneous (*C*) and miniature (*F*) synaptic currents by PD168077 in pyramidal neurons. (*G*,*H*,*J*,*K*) Representative traces of sEPSC (*G*), sIPSC (*H*), mEPSC (*J*), and mIPSC (*K*) before and after PD168077 (40 μM, 10 min) treatment in PV+ interneurons. Note, 2 time points (early: 3rd–5th min during PD application; late: 7th–10th min during PD application) were selected to show the biphasic effects of PD168077. Scale bars: 20 pA, 5 s (*G*,*H*), 2 s (*J*,*K*). (*I*,*L*) Bar graph summary of the percentage change in the spontaneous (*I*) and miniature (*L*) synaptic currents by PD168077 at 2 time points (early and late) in PV+ interneurons.

which was significantly attenuated by application of the D_4R antagonist L-745870 (20 μM) (37.6 ± 2.9%, $n = 11$, $P < 0.05$, K–W test, Fig. 7*E*), suggesting that D_4R-mediated reduction of sAP in pyramidal neurons partially mediates the reducing effect of dopamine. In PV+ interneurons (Fig. 7*C*,*D*), application of dopamine (1 μM, 10 min) induced a large increase of sAP frequency, and L-745870 (20 μM) significantly diminished the increasing effect at the early stage (DA: 10.5 ± 1.2-fold increase, DA + L745: 6.8 ± 0.8-fold increase, $n = 12$, $P < 0.05$, K–W test, Fig. 7*E*), suggesting that D_4R-mediated early increase of sAP in PV+ interneurons partially mediates the early effect of DA. Moreover, L-745870 prevented the reduction of sAP frequency after DA termination (DA: 7.4 ± 0.7-fold increase, $n = 10$, DA + L745: 11.8 ± 0.9-fold increase, $n = 12$, $P < 0.05$, K–W test, Fig. 7*E*), suggesting that D_4R-mediated late and sustained decrease of sAP in PV+ interneurons partially mediates the late effect of DA. Although dopamine (1 μM) produced strong effects on spontaneous AP frequency, it did not induce any effects on evoked AP frequency (Fig. 7*F*, pyramidal, $n = 8$; PV+, $n = 9$).

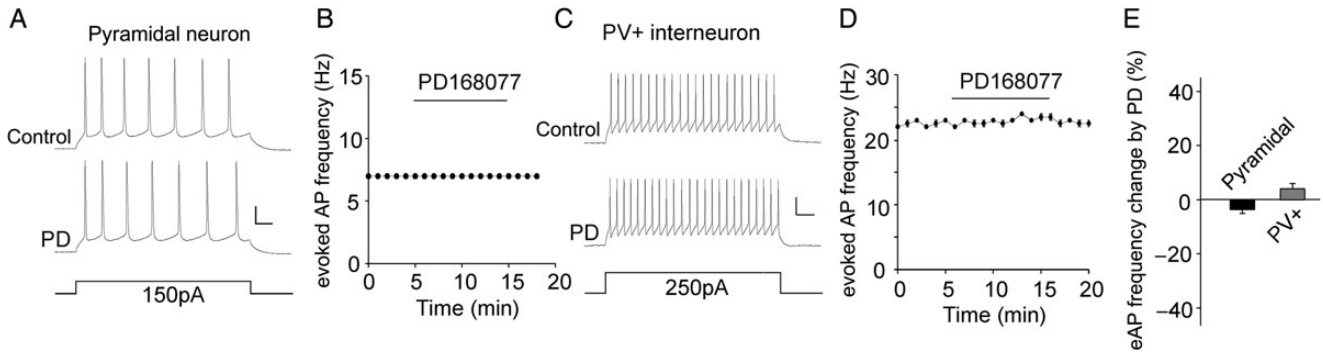

Figure 6. D_4R agonist PD168077 had not effect on the intrinsic excitability. (*A*,*C*) Representative traces of action potentials evoked by injected currents (20 s/pulse) before and after PD168077 (40 μM) application in a PFC pyramidal neuron (*A*) and a PV+ interneuron (*C*). Scale bars: 20 mV, 50 m. (*B*,*D*) The time course of evoked AP frequency showing the lack of effect of PD168077 in a PFC pyramidal neuron (*B*) and a PV+ interneuron (*D*). (*E*) Bar graph summary of the percentage change of evoked AP frequency by PD168077 in PFC pyramidal neurons and PV+ interneurons.

D4R Regulation of PFC Pyramidal Neurons and Parvalbumin-Positive Interneurons is Altered in the PCP Model of Schizophrenia

To test whether the physiological effects of D_4R activation are altered in neuropsychiatric disorders, we used the PCP model of schizophrenia. Mice were i.p. injected once daily with PCP (5 mg/kg) for 5 days. Subchronic administration of this dose of PCP to rodents induces a variety of behavioral and biochemical changes reminiscent of schizophrenia in humans (Jentsch et al. 1997, 1998; Adams and Moghaddam 1998; Moghaddam and Adams 1998), thus has been widely used as a pharmacological model of schizophrenia (Jentsch and Roth 1999). We first compared the excitability of PFC neurons in mice injected with saline versus PCP. No significant difference on sAP frequency was found in pyramidal neurons from saline- versus PCP-injected mice (saline: 1.1 ± 0.3 Hz, $n = 5$; PCP: 0.8 ± 0.5 Hz, $n = 5$, $P > 0.05$, K–W test). In PV+ interneurons from PCP-injected mice, sAP showed more clustered firing, but the overall sAP frequency was not significantly changed (saline: 2.5 ± 0.9 Hz, $n = 6$; PCP: 3.6 ± 1.3 Hz, $n = 6$, $P > 0.05$, K–W test).

Next, we compared the effects of PD16077 on sAP frequency in PFC neurons from mice injected with saline versus PCP. As shown in Figure 8, in pyramidal neurons, the decreasing effect of PD168077 on sAP frequency was significantly smaller in PCP-injected mice (saline: $76.8 \pm 7.9\%$, $n = 5$; PCP: $42.1 \pm 10.4\%$, $n = 6$, $P < 0.05$, K–W test). In PV+ interneurons, the early increasing effects of PD168077 on sAP frequency were unchanged (saline: $275.6 \pm 38.3\%$, $n = 5$; PCP: $282.8 \pm 44.3\%$, $n = 5$); however, the late decreasing effects of PD168077 on sAP frequency were significantly attenuated by PCP injection (saline: $68.6 \pm 9.8\%$, $n = 5$; PCP: $28.4 \pm 13.3\%$, $n = 5$, $P < 0.05$, K–W test).

Discussion

GABAergic interneurons in PFC are crucial for the gamma oscillations, which reflect the synchronization of pyramidal neuron activity during working memory, a major cognitive process subserved by PFC (Tallon-Baudry et al. 1998; Rao et al. 2000; Constantinidis et al. 2002; Howard et al. 2003). Fast-spiking PV-positive cells, the most prevalent interneuron subtype in neocortex, are robustly inhibited following activation of muscrinic, serotonin, adenosine, and $GABA_B$ receptors (Kruglikov and Rudy 2008). These neuromodulators, therefore, have a profound influence on the feedforward inhibition and rhythmic network activity. Dopamine D_4Rs are abundantly expressed in PFC GABAergic interneurons (Mrzljak et al. 1996); however, their functional role in this neuronal population has been largely unknown. In this study, we have found that D_4 receptor activation induces a fast and transient increase followed by a delayed decrease of the excitability of PV+ interneurons, which is distinct from its slow decreasing effect on the excitability of PFC pyramidal neurons. Since PV+ interneurons innervate the perisomatic region of pyramidal neurons and are responsible for the dominant part of the inhibition converging onto these projection neurons (Kawaguchi and Kubota 1993, 1998; Kruglikov and Rudy 2008), the D_4-R-induced initial increase of PV+ interneuron excitability could lead to the potent suppression of PFC network activity and output signal. At the later stage of D_4R activation, the decreased excitability of both PV+ interneurons and pyramidal neurons suggests that D_4 receptors serve as a key factor to dampen or balance the activity of PFC network. It provides a potential explanation for the cortical hyperexcitability exhibited in D_4R-deficient mice (Rubinstein et al. 2001).

Circuit excitability is driven by the integration of excitatory and inhibitory synaptic inputs (Maffei et al. 2004). We have found that the distinct effects of D_4R on sAP firing of PV+ interneurons and pyramidal neurons can be explained by the correlated changes on excitatory and inhibitory synaptic currents in response to D_4R activation in both cell types. Our previous studies have focused on the impact of D_4 receptors on glutamatergic and GABAergic synaptic transmission in PFC pyramidal neurons (Wang et al. 2002, 2003, 2006; Graziane et al. 2009; Yuen et al. 2010; Yuen and Yan 2011). In regular or high-activity PFC slices, a D_4R-mediated reduction of AMPAR-EPSC and $GABA_AR$-IPSC was often observed (Wang et al. 2002; Graziane et al. 2009; Yuen et al. 2010; Yuen and Yan 2011), consistent with the D_4R reduction of sEPSC, sIPSC, mEPSC, and mIPSC in PFC pyramidal neurons observed here. In PFC somatostatin-positive interneurons, we have found that D_4R activation induces a persistent depression of AMPAR transmission (Yuen and Yan 2009). Interestingly, D_4R induces biphasic effects on synaptic currents in PFC PV+ interneurons, with an initial sEPSC increase and sIPSC decrease and a delayed sEPSC decrease and sIPSC increase observed. The effects of D_4R on mEPSC and mIPSC suggest the involvement of pre- and/or post-synaptic

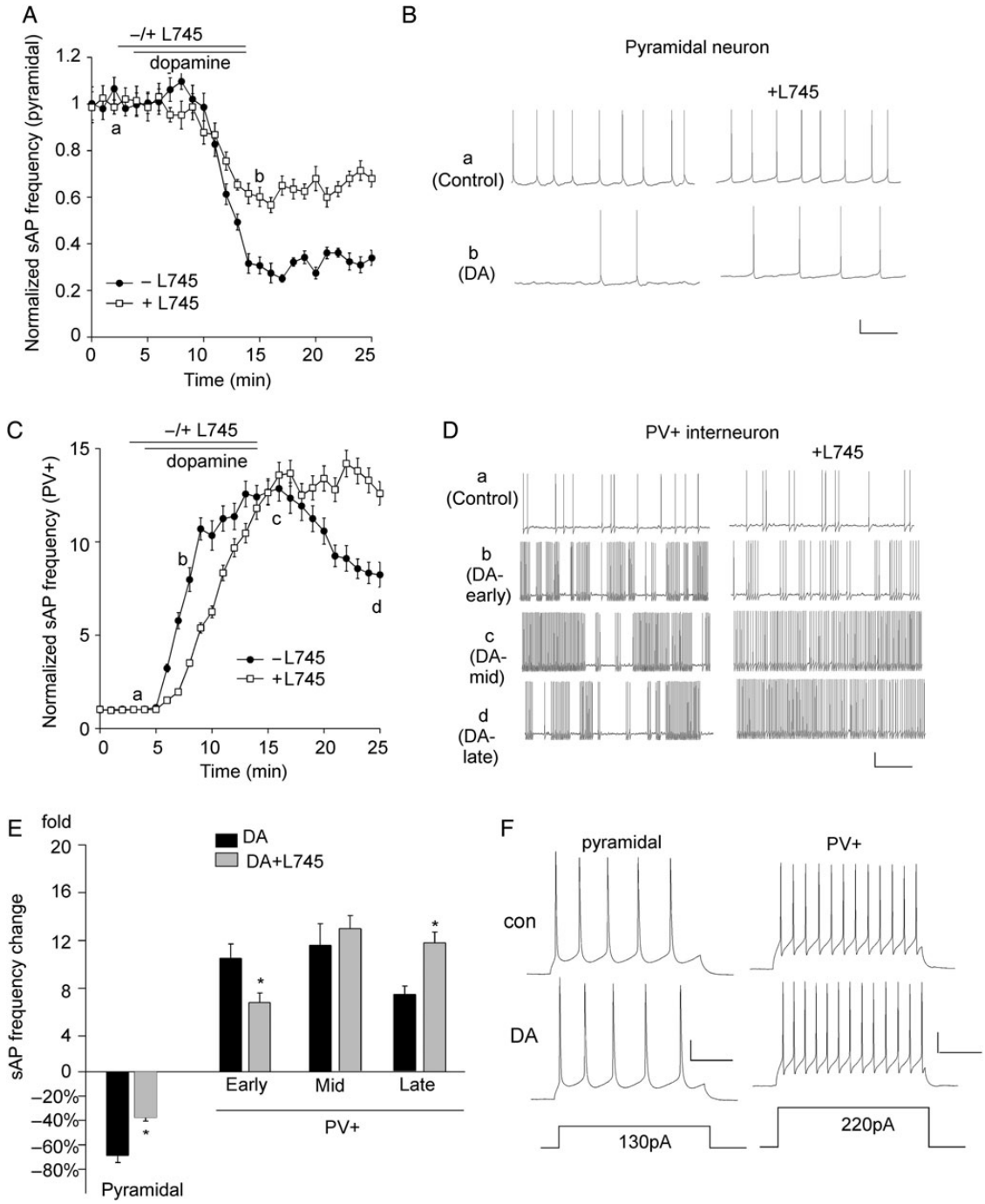

Figure 7. The effects of dopamine on sAP in PFC pyramidal neurons and PV+ interneurons are partially mediated by D4 receptors. (*A*) The time course of normalized sAP frequency showing the effect of dopamine (1 μM) in the absence (control) or presence of the D4 antagonist L745870 (20 μM) in PFC pyramidal neurons. (*B*) Representative traces of sAPs at different time points (denoted by *a*,*b*) in plot A. Scale bars: 20 mV, 1 s. (*C*) The time course of normalized sAP frequency showing the effect of dopamine (1 μM) in the absence (control) or presence of L745870 (20 μM) in PFC PV+ interneurons. (*D*) Representative traces of sAP at different time points (denoted by *a*–*d*) in plot C. Scale bars: 20 mV, 1 s. (*E*) Bar graph summary of the change in sAP frequency by dopamine in the absence or presence of L745870 in PFC pyramidal neurons and PV+ interneurons. The time-dependent effects of dopamine were analyzed in early (*b*), mid (*c*), and late (*d*) stages. $^*P < 0.05$. (*F*) Representative traces of action potentials evoked by injected currents (20 s/pulse) before and after dopamine (1 μM) application in a PFC pyramidal neuron and a PV+ interneuron. Scale bars: 20 mV, 100 ms.

mechanisms. One potential underlying mechanism could be the alteration of trafficking and function of postsynaptic AMPA and $GABA_A$ receptors by D_4R signaling involving kinases/phosphatases and cytoskeleton proteins (Wang et al. 2002; Graziane et al. 2009; Yuen and Yan 2009, 2011; Yuen et al. 2010). Alternatively, D_4R-induced changes in presynaptic release of glutamate and GABA due to the regulation of specific K^+ channels and/or Ca^{2+} channels (Pillai et al. 1998; Wilke et al. 1998; Ramanathan et al. 2008) may also play an important role here.

Given that D_4Rs presumably act together with all other dopamine receptors, we performed experiments with dopamine application to assess how much of the neuronal excitability is associated with D_4R activation. Surprisingly, application of a low dose of dopamine (1 uM) induced a large (~70%)

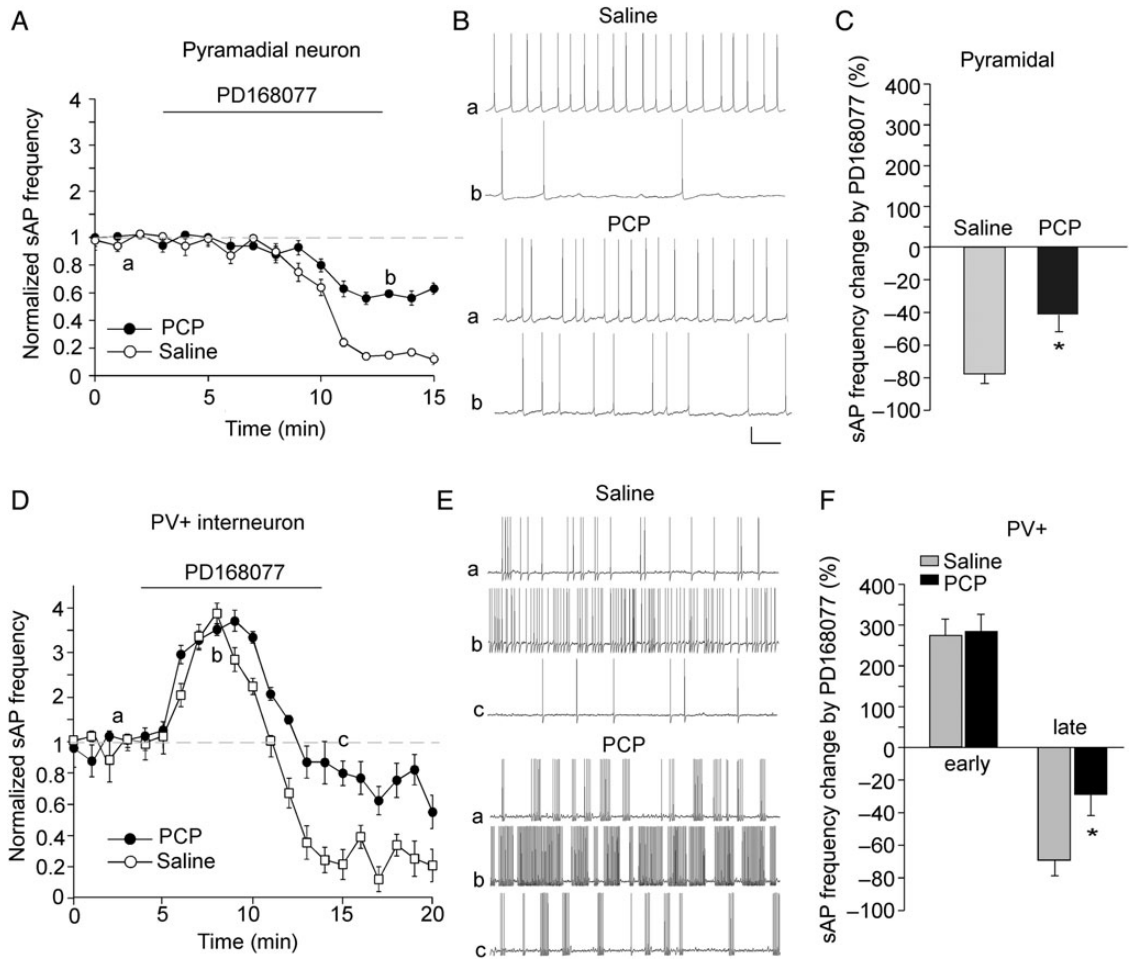

Figure 8. The effects of D_4R on sAP frequency in PFC pyramidal neurons and PV+ interneurons were altered in the PCP model of schizophrenia. (*A*,*D*) The plot of normalized sAP frequency showing the effect of PD168077 in pyramidal neurons (*A*) and PV+ interneurons (*D*) from saline- versus PCP (5 mg/kg, 3-day)-injected mice. (*B*,*E*) Representative sAP traces at different time points (denoted by *a*–*c* in plots *A*,*D*) in pyramidal neurons (*B*) and PV+ interneuron (*E*) from saline- versus PCP-injected mice. Scale bars: 20 mV, 1 s. (*C*,*F*) Bar graph summary of the percentage change in sAP frequency by PD168077 in pyramidal neurons (*C*) and PV+ interneurons (*F*) from saline- versus PCP-injected mice. $^*P < 0.05$.

decrease of sAP frequency in PFC pyramidal neurons and a huge (~10-fold) increase of sAP frequency in PV+ interneurons, whereas it failed to alter evoked AP in either cell type. It suggests that the low dose of dopamine mainly affects synaptically driven excitability in PFC neurons. Blocking D_4Rs significantly attenuated the decreasing effect of dopamine on sAP in PFC pyramidal neurons, and the increasing effect of dopamine on sAP at the early and late stages in PV+ interneurons, suggesting the important involvement of D_4Rs in the action of dopamine.

Alterations in both pre- and post-synaptic markers of the strength of GABAergic inputs from PV+ neurons to pyramidal neurons have been discovered in PFC of subjects with schizophrenia (Lewis et al. 2011). Physiological changes in both cell types in schizophrenia conditions are not well known. In this study, we have found altered effects of D_4R on the excitability of these neurons from a model of schizophrenia. While the transient increasing effect of D_4R in PV+ interneurons is intact, the delayed decreasing effect of D_4R in both cell types is significantly lost. These alterations may contribute to the aberrant activity of PFC circuits and impaired gamma oscillations in schizophrenia (Uhlhaas and Singer 2006; Frantseva et al. 2012; Lewis et al. 2012). In summary, our results have demonstrated that the glutamatergic synapse—whether from pyramidal neuron to pyramidal neuron or from pyramidal neuron to interneuron—is a crucial point of action of the D_4 receptors.

Authors' Contributions

Ping Zhong and Zhen Yan conceived and designed the experiments and contributed to reagents/materials/analysis tools. Ping Zhong performed the experiments and analyzed the data. Zhen Yan wrote the manuscript.

Funding

This work was supported by NIH grant DA037618 and VA Merit Award 1I01BX001633 to ZY.

Notes

We thank X. Chen for excellent technical support. *Conflict of Interest*: None declared.

References

Adams B, Moghaddam B. 1998. Corticolimbic dopamine neurotransmission is temporally dissociated from the cognitive and locomotor effects of phencyclidine. J Neurosci. 18:5545–5554.

Akbarian S, Kim JJ, Potkin SG, Hagman JO, Tafazzoli A, Bunney WE Jr, Jones EG. 1995. Gene expression for glutamic acid decarboxylase is reduced without loss of neurons in prefrontal cortex of schizophrenics. Arch Gen Psychiatry. 52:258–266.

Arvanov VL, Wang RY. 1999. Clozapine, but not haloperidol, prevents the functional hyperactivity of *n*-methyl-d-aspartate receptors in rat cortical neurons induced by subchronic administration of phencyclidine. J Pharmacol Exp Ther. 289:1000–1006.

Beasley CL, Zhang ZJ, Patten I, Reynolds GP. 2002. Selective deficits in prefrontal cortical GABAergic neurons in schizophrenia defined by the presence of calcium-binding proteins. Biol Psychiatry. 52: 708–715.

Beierlein M, Gibson JR, Connos BW. 2003. Two dynamically distinct inhibitory networks in layer 4 of the neocortex. J Neurophysiol. 90:2987–3000.

Cauli B, Audinat E, Lambolez B, Angulo MC, Ropert N, Tsuzuki K, Hestrin S, Rossier J. 1997. Molecular and physiological diversity of cortical nonpyramidal cells. J Neurosci. 17:3894–3906.

Chattopadhyaya B, Cristo GD, Higashiyama H, Knott GW, Kuhlman SJ. 2004. Experience and activity-dependent maturation of perisomatic GABAergic innervation in primary visual cortex during a postnatal critical period. J Neurosci. 24:9598–9611.

Constantinidis C, Williams GV, Goldman-Rakic PS. 2002. A role for inhibition in shaping the temporal flow of information in prefrontal cortex. Nat Neurosci. 5:175–180.

Cruikshank SJ, Lewis TJ, Connors BW. 2007. Synaptic basis for intense thalamocortical activation of feedforward inhibitory cells in neocortex. Nat Neurosci. 10:462–468.

El-Faddagh M, Laucht M, Maras A, Vöhringer L, Schmidt MH. 2004. Association of dopamine D4 receptor (DRD4) gene with attention-deficit/hyperactivity disorder (ADHD) in a high-risk community sample: a longitudinal study from birth to 11 years of age. J Neural Transm. 111:883–889.

Frantseva M, Cui J, Farzan F, Chinta LV, Perez Velazquez JL, Daskalakis ZJ. 2012. Disrupted cortical conductivity in schizophrenia: TMS-EEG Study. Cereb Cortex. 24:211–221.

Galarreta M, Hestrin S. 1999. A network of fast-spiking cells in the neocortex connected by electrical synapses. Nature. 402:72–75.

Geiger JR, Melcher T, Koh DS, Sakmann B, Seeburg PH, Jonas P, Monyer H. 1995. Relative abundance of subunit mRNAs determines gating and Ca2+ permeability of AMPA receptors in principal neurons and interneurons in rat CNS. Neuron. 15:193–204.

Gibson JR, Huber KM, Sudhof TC. 2009. Neuroligin-2 deletion selectively decreases inhibitory synaptic transmission originating from fast-spiking but not from somatostatin-positive interneurons. J Neurosci. 29:13883–13897.

Graziane NM, Yuen EY, Yan Z. 2009. Dopamine D4 receptors regulate GABAA receptor trafficking via an actin/cofilin/myosin-dependent mechanism. J Biol Chem. 284:8329–8336.

Hashimoto T, Volk DW, Eggan SM, Mirnics K, Pierri JN, Sun Z, Sampson AR, Lewis DA. 2003. Gene expression deficits in a subclass of GABA neurons in the prefrontal cortex of subjects with schizophrenia. J Neurosci. 23:6315–6326.

Hendry SH, Schwark HD, Jones EG, Yan J. 1987. Numbers and proportions of GABA-immunoreactive neurons in different areas of monkey cerebral cortex. J Neurosci. 7:1503–1519.

Hestrin S. 1993. Different glutamate receptor channels mediate fast excitatory synaptic currents in inhibitory and excitatory cortical neurons. Neuron. 11:1083–1091.

Howard MW, Rizzuto DS, Caplan JB, Madsen JR, Lisman J, Aschenbrenner-Scheibe R, Schulze-Bonhage A, Kahana MJ. 2003. Gamma oscillations correlate with working memory load in humans. Cereb Cortex. 13:1369–1374.

Javitt DC, Zukin SR. 1991. Recent advances in the phencyclidine model of schizophrenia. Am J Psychiatry. 148:1301–1308.

Jentsch JD, Roth RH. 1999. The neuropsychopharmacology of phencyclidine: from NMDA receptor hypofunction to the dopamine hypothesis of schizophrenia. Neuropsychopharmacology. 20: 201–225.

Jentsch JD, Tran A, Le D, Youngren KD, Roth RH. 1997. Subchronic phencyclidine administration reduces mesoprefrontal dopamine utilization and impairs prefrontal cortical-dependent cognition in the rat. Neuropsychopharmacology. 17:92–99.

Jentsch JD, Tran A, Taylor JR, Roth RH. 1998. Prefrontal cortical involvement in phencyclidine-induced activation of the mesolimbic dopamine system: behavioral and neurochemical evidence. Psychopharmacology (Berl). 138:89–95.

Kapur S, Remington G. 2001. Atypical antipsychotics: new directions and new challenges in the treatment of schizophrenia. Annu Rev Med. 52:503–517.

Kawaguchi Y. 1995. Physiological subgroups of nonpyramidal cells with specific morphological characteristic in layer 2/3 of rat frontal cortex. J Neurosci. 15:2638–2655.

Kawaguchi Y, Kubota Y. 1993. Correlation of physiological subgroupings of nonpyramidal cells with parvalbumin- and calbindinD28k-immunoreactive neurons in layer V of rat frontal cortex. J Neurophysiol. 70:387–396.

Kawaguchi Y, Kubota Y. 1997. GABAergic cell subtypes and their synaptic connections in rat frontal cortex. Creb Cortex. 7:476–486.

Kawaguchi Y, Kubota Y. 1998. Neurochemical features and synaptic connections of large physiologically-identified GABAergic cells in the rat frontal cortex. Neuroscience. 85:677–701.

Kruglikov I, Rudy B. 2008. Perisomatic GABA release and thalamocortical integration onto neocortical excitatory cells are regulated by neuromodulators. Neuron. 58:911–924.

LaHoste GJ, Swanson JM, Wigal SB, Glabe C, Wigal T, King N, Kennedy JL. 1996. Dopamine D4 receptor gene polymorphism is associated with attention deficit hyperactivity disorder. Mol Psychiatry. 1:121–124.

Levitt P, Eagleson KL, Powell EM. 2004. Regulation of neocortical interneuron development and the implications for neurodevelopmental disorders. Trends Neurosci. 27:400–406.

Lewis DA, Curley AA, Glausier JR, Volk DW. 2012. Cortical parvalbumin interneurons and cognitive dysfunction in schizophrenia. Trends Neurosci. 35:57–67.

Lewis DA, Fish KN, Arion D, Gonzalez-Burgos G. 2011. Perisomatic inhibition and cortical circuit dysfunction in schizophrenia. Curr Opin Neurobiol. 21:866–872.

Lewis DA, Hashimoto T, Volk DW. 2005. Cortical inhibitory neurons and schizophrenia. Nat Rev Neurosci. 6:312–324.

Li D, Sham PC, Owen MJ, He L. 2006. Meta-analysis shows significant association between dopamine system genes and attention deficit hyperactivity disorder (ADHD). Hum Mol Genet. 15:2276–2284.

Maffei A, Nelson SB, Turigiano GG. 2004. Selective reconfiguration of layer 4 visual cortical circuitry by visual deprivation. Nat Neurosci. 7:1353–1359.

Maffei A, Turigiano GG. 2008. Multiple modes of network homeostasis in visual cortical layer 2/3. J Neurosci. 28:4377–4384.

Markram H, Toledo-Rodriguez M, Wang Y, Gupta A, Silberberg G, Wu C. 2004. Interneurons of the neocortical inhibitory system. Nat Rev Neurosci. 5:793–807.

McBain CJ, Fisahn A. 2001. Interneurons unbound. Nat Rev Neurosci. 2:11–23.

Moghaddam B, Adams BW. 1998. Reversal of phencyclidine effects by a group II metabotropic glutamate receptor agonist in rats. Science. 281:1349–1352.

Mrzljak L, Bergson C, Pappy M, Huff R, Levenson R, Goldman-Rakic PS. 1996. Localization of dopamine D4 receptors in GABAergic neurons of the primate brain. Nature. 381:245–248.

Okaty BW, Miller MN, Sugino K, Hempel CM, Nelson SB. 2009. Transcriptional and electrophysiological maturation of neocortical fast-spiking GABAergic interneurons. J Neurosci. 29:7040–7052.

Pillai G, Brown NA, McAllister G, Milligan G, Seabrook GR. 1998. Human D2 and D4 dopamine receptors couple through betagamma G-protein subunits to inwardly rectifying K+ channels (GIRK1) in a Xenopus oocyte expression system: selective antagonism by L-741,626 and L-745,870 respectively. Neuropharmacology. 37:983–987.

Ramanathan S, Tkatch T, Atherton JF, Wilson CJ, Bevan MD. 2008. D2-like dopamine receptors modulate SKCa channel function in subthalamic nucleus neurons through inhibition of Cav2.2 channels. J Neurophysiol. 99:442–459.

Rao SG, Williams GV, Goldman-Rakic PS. 2000. Destruction and creation of spatial tuning by disinhibition: GABA(A) blockade of prefrontal cortical neurons engaged by working memory. J Neurosci. 20:485–494.

Rowe DC, Stever C, Giedinghagen LN, Gard JM, Cleveland HH, Terris ST, Mohr JH, Sherman S, Abramowitz A, Waldman ID. 1998. Dopamine DRD4 receptor polymorphism and attention deficit hyperactivity disorder. Mol Psychiatry. 3:419–426.

Rubinstein M, Cepeda C, Hurst RS, Flores-Hernandez J, Ariano MA, Falzone TL, Kozell LB, Meshul CK, Bunzow JR, Low MJ et al. 2001. Dopamine D4 receptor-deficient mice display cortical hyperexcitability. J Neurosci. 21:3756–3763.

Rubinstein M, Phillips TJ, Bunzow JR, Falzone TL, Dziewczapolski G, Zhang G, Fang Y, Larson JL, McDougall JA, Chester JA et al. 1997. Mice lacking dopamine D4 receptors are supersensitive to ethanol, cocaine, and methamphetamine. Cell. 90:991–1001.

Sanchez-Vives MV, McCormick DA. 2000. Cellular and network mechanisms of rhythmic recurrent activity in neocortex. Nat Neurosci. 3:1027–1034.

Sawaguchi T, Goldman-Rakic PS. 1991. D1 dopamine receptors in prefrontal cortex: involvement in working memory. Science. 251:947–950.

Spencer KM, Nestor PG, Niznikiewicz MA, Salisbury DF, Shenton ME, McCarley RW. 2003. Abnormal neural synchrony in schizophrenia. J Neurosci. 23:7407–7411.

Tallon-Baudry C, Bertrand O, Peronnet F, Pernier J. 1998. Induced gamma-band activity during the delay of a visual short-term memory task in humans. J Neurosci. 18:4244–4254.

Torrey EF, Barci BM, Webster MJ, Bartko JJ, Meador-Woodruff JH, Knable MB. 2005. Neurochemical markers for schizophrenia, bipolar disorder, and major depression in postmortem brains. Biol Psychiatry. 57:252–260.

Uhlhaas PJ, Singer W. 2006. Neural synchrony in brain disorders: relevance for cognitive dysfunctions and pathophysiology. Neuron. 52:155–168.

Van Tol HH, Bunzow JR, Guan HC, Sunahara RK, Seeman P, Niznik HB, Civelli O. 1991. Cloning of the gene for a human dopamine D4 receptor with high affinity for the antipsychotic clozapine. Nature. 350:610–614.

Vijayraghavan S, Wang M, Birnbaum SG, Williams GV, Arnsten AF. 2007. Inverted-U dopamine D1 receptor actions on prefrontal neurons engaged in working memory. Nat Neurosci. 10:376–384.

Volk DW, Austin MC, Pierri JN, Sampson AR, Lewis DA. 2000. Decreased glutamic acid decarboxylase67 messenger RNA expression in a subset of prefrontal cortical gamma-aminobutyric acid neurons in subjects with schizophrenia. Arch Gen Psychiatry. 57:237–245.

Volk DW, Pierri JN, Fritschy JM, Auh S, Sampson AR, Lewis DA. 2002. Reciprocal alterations in pre- and postsynaptic inhibitory markers at chandelier cell inputs to pyramidal neurons in schizophrenia. Cereb Cortex. 12:1063–1070.

Walsh CA, Morrow EM, Rubenstein JL. 2008. Autism and brain development. Cell. 135:396–400.

Wang M, Vijayraghavan S, Goldman-Rakic PS. 2004. Selective D2 receptor actions on the functional circuitry of working memory. Science. 303:853–856.

Wang X, Gu Z, Zhong P, Chen G, Feng J, Yan Z. 2006. Aberrant regulation of NMDA receptors by dopamine D4 signaling in rats after phencyclidine exposure. Mol Cell Neurosci. 31:15–25.

Wang X, Zhong P, Gu Z, Yan Z. 2003. Regulation of NMDA receptors by dopamine D4 signaling in prefrontal cortex. J Neurosci. 23:9852–9861.

Wang X, Zhong P, Yan Z. 2002. Dopamine D4 receptors modulate GABAergic signaling in pyramidal neurons of prefrontal cortex. J Neurosci. 22:9185–9193.

Wedzony K, Chocyk A, Mackowiak M, Fijal K, Czyrak A. 2000. Cortical localization of dopamine D4 receptors in the rat brain – immunocytochemical study. J Physiol Pharmacol. 51:205–221.

Wilke RA, Hsu SF, Jackson MB. 1998. Dopamine D4 receptor mediated inhibition of potassium current in neurohypophysial nerve terminals. J Pharmacol Exp Ther. 284:542–548.

Williams GV, Goldman-Rakic PS. 1995. Modulation of memory fields by dopamine D1 receptors in prefrontal cortex. Nature. 376:572–575.

Woo TU, Whitehead RE, Melchitzky DS, Lewis DA. 1998. A subclass of prefrontal gamma-aminobutyric acid axon terminals are selectively altered in schizophrenia. Proc Natl Acad Sci USA. 95:5341–5346.

Yang CR, Seamans JK, Gorlova N. 1996. Electrophysiological and morphological properties of layers V-VI principal cells in rat prefrontal cortex *in Vitro*. J Neurosci. 16:1904–1921.

Yuen EY, Yan Z. 2011. Cellular mechanisms for dopamine D4 receptor-induced homeostatic regulation of alpha-amino-3-hydroxy-5-methyl-4-isoxazolepropionic acid (AMPA) receptors. J Biol Chem. 286:24957–24965.

Yuen EY, Yan Z. 2009. Dopamine D4 receptors regulate AMPA receptor trafficking and glutamatergic transmission in GABAergic interneurons of prefrontal cortex. J Neurosci. 29:550–562.

Yuen EY, Zhong P, Yan Z. 2010. Homeostatic regulation of glutamatergic transmission by dopamine D4 receptors. Proc Natl Acad Sci USA. 107:22308–22313.

Zhong P, Gu Z, Wang X, Jiang H, Feng J, Yan Z. 2003. Impaired modulation of GABAergic transmission by muscarinic receptors in a mouse transgenic model of Alzheimer's disease. J Biol Chem. 278:26888–26896.